JCI The Journal of Clinical Investigation

Analysis of mutations from SCID and Omenn syndrome patients reveals the central role of the Rag2 PHD domain in regulating V(D)J recombination

Chrystelle Couëdel, … , Anna Villa, Patricia Cortes

J Clin Invest. 2010;120(4):1337-1344. https://doi.org/10.1172/JCI41305.

Research Article **Immunology**

Rag2 plays an essential role in the generation of antigen receptors. Mutations that impair Rag2 function can lead to severe combined immunodeficiency (SCID), a condition characterized by complete absence of T and B cells, or Omenn syndrome (OS), a form of SCID characterized by the virtual absence of B cells and the presence of oligoclonal autoreactive T cells. Here, we present a comparative study of a panel of mutations that were identified in the noncanonical plant homeodomain (PHD) of Rag2 in patients with SCID or OS. We show that PHD mutant mouse Rag2 proteins that correspond to those found in these patients greatly impaired endogenous recombination of Ig gene segments in a Rag2-deficient pro-B cell line and that this correlated with decreased protein stability, impaired nuclear localization, and/or loss of the interaction between Rag2 and core histones. Our results demonstrate that point mutations in the PHD of Rag2 compromise the functionality of the entire protein, thus explaining why the phenotype of cells expressing PHD point mutants differs from those expressing core Rag2 protein that lacks the entire C-terminal region and is therefore devoid of the regulation imposed by the PHD. Together, our findings reveal the various deleterious effects of PHD Rag2 mutations and demonstrate the crucial role of this domain in regulating antigen receptor gene assembly. We believe these results […]

Analysis of mutations from SCID and Omenn syndrome patients reveals the central role of the Rag2 PHD domain in regulating V(D)J recombination

Chrystelle Couëdel,[1] Christopher Roman,[2] Alison Jones,[3] Paolo Vezzoni,[4,5] Anna Villa,[4,5] and Patricia Cortes[1]

[1]Immunology Institute, Department of Medicine, Mount Sinai School of Medicine, New York, New York. [2]Program in Molecular and Cellular Biology, School of Graduate Studies, State University of New York — Downstate Medical Center at Brooklyn, New York. [3]Immunology Department, Great Ormond Street Hospital, London, United Kingdom. [4]Istituto Clinico Humanitas ORCCS, Rozzano, Italy. [5]Istituto di Tecnologie Biomediche, Consiglio Nazionale delle Ricerche, Segrate, Italy.

Rag2 plays an essential role in the generation of antigen receptors. Mutations that impair Rag2 function can lead to severe combined immunodeficiency (SCID), a condition characterized by complete absence of T and B cells, or Omenn syndrome (OS), a form of SCID characterized by the virtual absence of B cells and the presence of oligoclonal autoreactive T cells. Here, we present a comparative study of a panel of mutations that were identified in the noncanonical plant homeodomain (PHD) of Rag2 in patients with SCID or OS. We show that PHD mutant mouse Rag2 proteins that correspond to those found in these patients greatly impaired endogenous recombination of Ig gene segments in a Rag2-deficient pro-B cell line and that this correlated with decreased protein stability, impaired nuclear localization, and/or loss of the interaction between Rag2 and core histones. Our results demonstrate that point mutations in the PHD of Rag2 compromise the functionality of the entire protein, thus explaining why the phenotype of cells expressing PHD point mutants differs from those expressing core Rag2 protein that lacks the entire C-terminal region and is therefore devoid of the regulation imposed by the PHD. Together, our findings reveal the various deleterious effects of PHD Rag2 mutations and demonstrate the crucial role of this domain in regulating antigen receptor gene assembly. We believe these results reveal new mechanisms of immunodeficiency in SCID and OS.

Introduction

V(D)J recombination is the site-specific DNA rearrangement process that assembles the B cell receptor and TCR genes during lymphoid development. Recombination is initiated by the lymphoid-specific Rag1 and Rag2 recombinase (1, 2), which introduces double-strand DNA breaks at recombination signal sequences (RSSs) flanking variable (V), diversity (D), and junction (J) gene segments spread along the Ig and TCR loci. Subsequently, the ubiquitous nonhomologous end-joining (NHEJ) machinery, which includes Ku70/Ku80, DNA-PKcs, Artemis, XRCC4, LigaseIV, and Cernunnos-XLF, repairs those lesions to form V(D)J coding joints and signal joints (3, 4). The recombination process is tightly regulated, occurring at specific stages of development and in specific cell types (e.g., Ig and TCR genes are rearranged in B and T cells, respectively). This process takes place in a temporal manner, with Ig heavy chain rearrangements preceding Ig light chain rearrangements and D-to-J rearrangements preceding V-to-DJ rearrangements (5).

V(D)J recombination is critical for proper immune function and, when impaired, generally results in the arrest of both B and T cell development, leading to severe combined immunodeficiency (SCID). Accordingly, mutations in Rag1, Rag2, or NHEJ factors have been described in patients characterized by a complete absence of T and B cells (T-B-SCID). Hypomorphic mutations in Rag1, Rag2, and Artemis or LigaseIV have also been described in patients diagnosed with Omenn syndrome (OS) (6–8), another SCID condition characterized by the virtual absence of B cells despite a high level of serum IgE, the presence of oligoclonal autoreactive T cells, recurrent severe infections, and particular clinical features, such as erythrodermia, hepatosplenomegaly, protracted diarrhea, and failure to thrive. Numerous T-B-SCID and OS cases have been associated with mutations in Rag1 and Rag2 proteins (9).

Deletion analyses defined core regions for both Rag1 (aa 384–1,008 out of 1,040 aa) and Rag2 (aa 1–382 out of 527 aa) that are necessary and sufficient for recombination of exogenous plasmid V(D)J recombination substrates in nonlymphoid cells (10–12). The core proteins have been widely used in vitro to reveal the biochemistry of the recombination reaction due to technical difficulties in purification of their full-length Rag1 and Rag2 counterparts. For example, core Rag1 is indeed crucial for V(D)J recombination, as it contains the catalytic site for DNA cleavage (13) and mediates the main contacts with the RSSs (14). Similarly, core Rag2 assists Rag1 interaction with the RSS and is essential for DNA distortion during catalysis (14). However, the non-core regions of Rag1 and Rag2 are evolutionary conserved, and several studies suggest that they have important in vivo functions (15). Indeed, it was shown in B cells that the C-terminal region of Rag2 was important for IgH V-to-DJ rearrangement (16). The C terminus of Rag2 includes a hinge domain, with a

Conflict of interest: The authors have declared that no conflict of interest exists.

Citation for this article: *J Clin Invest.* 2010;120(4):1337–1344. doi:10.1172/JCI41305.

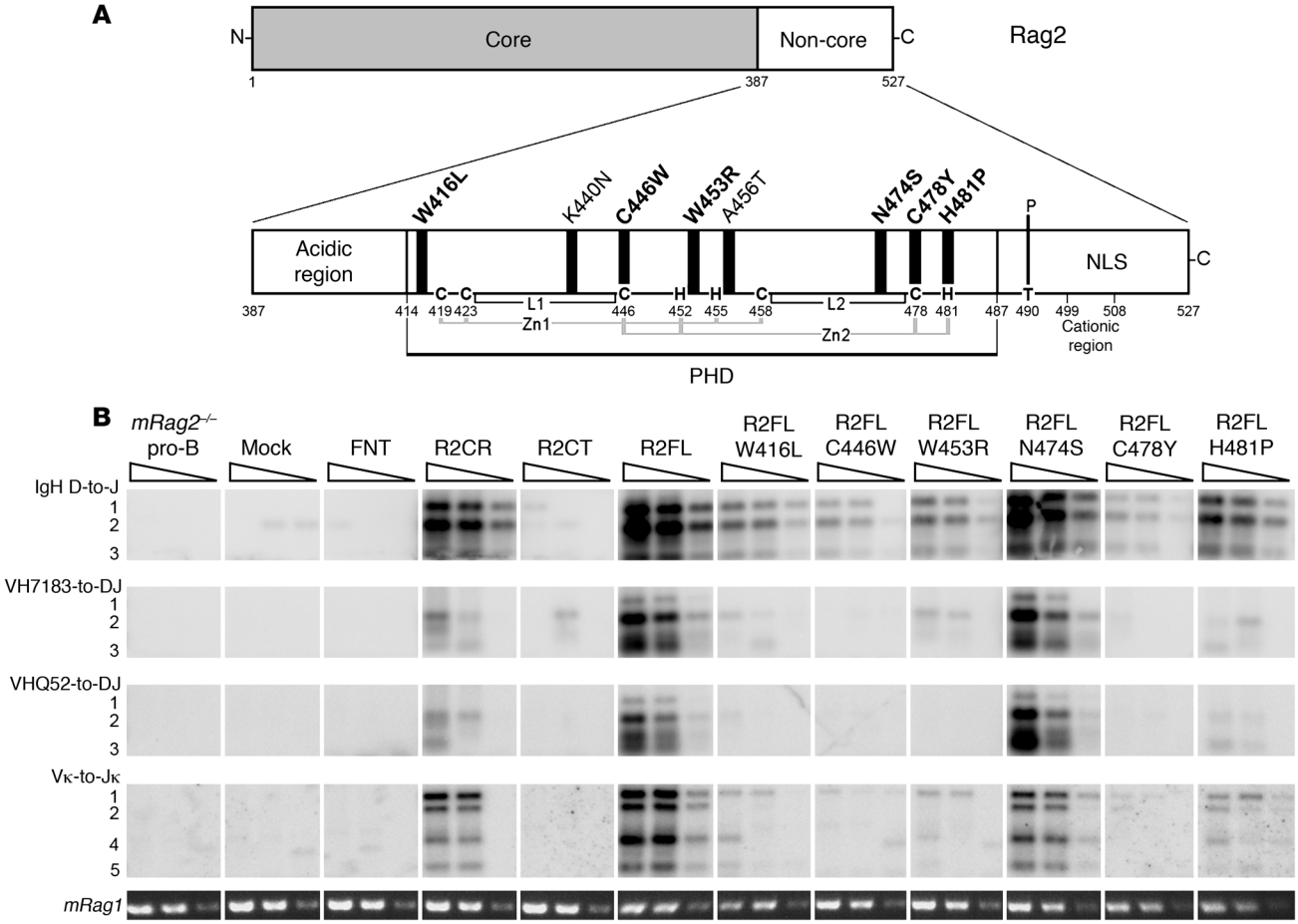

Figure 1

T-B-SCID/OS $Rag2_{PHD}$ mutants fail to support recombination at the endogenous Ig loci. (**A**) Schematic of the Rag2 protein showing the core and non-core regions and enhancement of the C-terminal non-core region that includes the acidic hinge region, the PHD, and the noncanonical NLS overlapping the phosphorylation site at residue T490 (thin black vertical bar) and the cationic region between residues 499–508. Thick black vertical bars indicate residues mutated in OS/SCID patients; mutations analyzed in this study are in bold. Anchor residues forming the noncanonical PHD finger are indicated, and related interactions with Zinc ions (Zn1 and Zn2) are represented by gray bars; L1 and L2 indicate segments forming loops between pairs of zinc-coordinating residues, as previously described (18). C and H represent Zn^{+2} coordinating cysteine and histidine residues present in the Rag2 PHD domain. (**B**) A mouse *Rag2*$^{-/-}$ pro-B cell line was retrovirally transduced and selected to express constructs of interest: empty vector (Mock), FNT tag, FNT-tagged R2CR, C terminus of Rag2 (R2CT), R2FL, or full-length T-B-SCID/OS Rag2 mutants. Genomic DNA was harvested from the above cell lines, and Southern Blot analysis was performed on PCR-amplified products of IgH D-to-J, VH7183-to-DJ, VHQ52-to-DJ, and Vκ-to-Jκ rearrangements, as indicated to the left of each panel. Numbers of the left side of the figure (1 to 5) represent different recombination products. Triangles at the top of panels indicate PCR amplification of 400 ng, 200 ng, and 25 ng of DNA template. A fragment of *Rag1* gene was amplified as a loading control. For each type of rearrangement, samples were loaded on the same gel, and detection intensity was identical. PCR from nontransduced cells was also used as control. The results shown are representative of 2 independent experiments. *mRag2*$^{-/-}$, mouse *Rag2*$^{-/-}$.

high percentage of acidic aa, that connects the core region to a noncanonical plant homeodomain (PHD) finger (17, 18) and a noncanonical nuclear localization signal (NLS) (19), which overlaps a phosphorylation site at residue T490 and a cationic region implicated in the cell-cycle regulated degradation of Rag2 (20–23). Our group has reported the crucial role of the C-terminal region of Rag2 in interacting with histones (24). Our study focused on point mutations in the acidic region of Rag2 that abolished the interaction with histones and impaired the completion of V(D)J rearrangements on endogenous Ig loci. More recently, the PHD domain of Rag2 ($Rag2_{PHD}$) was shown to interact with hypermethylated histone H3 and mutations described in SCID/OS (specifically W453R), abolish this interaction, and greatly impair recombination (25–27). Moreover, a recent study also indicates that a histone H3 peptide trimethylated in lysine 4 stimulates Rag enzymatic activity in vitro, and this stimulation is specifically abolished by the W453R mutation (28).

Here, we present a comparative analysis of several known $Rag2_{PHD}$ mutations reported in SCID and/or OS patients to better understand how this region controls Rag2 function. We find that not only can some of these mutations disrupt Rag2 association with the histones but also show that they can severely impair Rag2 stability or impede its nuclear localization, either of which appears to be the first barrier against effective function.

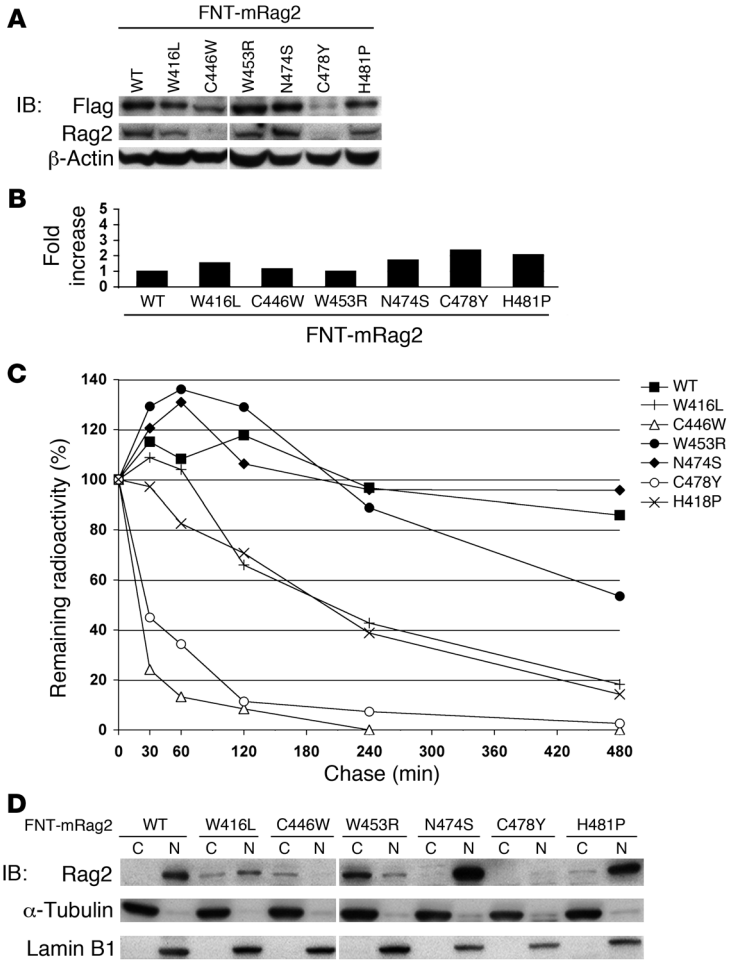

Figure 2

T-B-SCID/OS $Rag2_{PHD}$ mutations affect Rag2 stability and cellular localization in pro-B cells. A mouse *Rag2*$^{-/-}$ pro-B cell line was retrovirally transduced to express FNT-tagged full-length wild-type Rag2 or T-B-SCID/OS mutants. (**A**) Western blot analysis was performed on whole cell extracts from retrovirally transduced pro-B cell lines for Flag, Rag2, and β-actin. Samples were loaded on the same gel, and the length of exposure was identical. The vertical line between FNT–mouse Rag2–C446W and –W453R mutants indicates a sample that was excluded from our study. (**B**) Total mRNA was isolated from retrovirally transduced pro-B cell lines, and Rag2 transcription levels were determined by Q-PCR. The average of 2 independent experiments are graphed as fold increase compared with mRNA expression of FNT–mouse Rag2. (**C**) Retrovirally transduced pro-B cell lines were pulse labeled with [^{35}S] methionine/cysteine to determine degradation of wild-type Rag2 and T-B-SCID/OS mutants. Radiolabeled proteins were IP at various times after pulse with anti-Rag2 antibody, fractionated by SDS PAGE, and quantified on a PhosphorImager. Data were normalized to the radioactivity levels at the end of pulse. The graph presents the average from 2 independent experiments. (**D**) Cellular localization of Rag2 in retrovirally transduced pro-B cell lines was determined by Western blotting analysis of fractionated cytoplasm (C) and nuclear (N) extracts (top). Purity and loading of the fractions were analyzed by Western blotting for α-tubulin (middle) and Lamin B1 (bottom). The vertical line between FNT–mouse Rag2–C446W and –W453R is as in **A**.

Results

SCID/OS $Rag2_{PHD}$ mutations impair recombination at the endogenous Ig loci. To date, 7 mutations leading to human SCID and/or OS have been mapped outside the core region of Rag2: W416L, K440N, W453R, A456T, N474S, C478Y, and H481P (9, 18, 29–33). C446W, identified in a patient that was diagnosed with T-B-SCID, is a new mutation to our knowledge and is included in this study (A. Villa, unpublished observations). Interestingly, all SCID/OS mutations in the non-core region of Rag2 localize within the PHD finger (Figure 1A), supporting the idea that this domain has a crucial role in Rag2 essential functions during V(D)J recombination.

We investigated the effect of 6 of the $Rag2_{PHD}$ mutations on endogenous V(D)J recombination by expressing the wild-type and mutated Rag2 proteins in Abelson-transformed *Rag2*$^{-/-}$ pro-B cells in which the Ig loci are in germline configuration. We generated a panel of 6 full-length mouse Rag2 mutants, with each representing 1 mutation (W416L, C446W, W453R, N474S, C478Y, and H481P) within the PHD domain. K440N and A456T were not investigated in this study. Wild-type and mutant Rag2 proteins were tagged with Flag-NLS-thioredoxin (FNT). The murine *Rag2*$^{-/-}$ pro-B cell line was transduced with either control retrovirus carrying only the FNT tag or retroviruses carrying the genes encoding the tagged wild-type Rag2 or Rag2 mutants, as previously described (24). Eleven separate B cell lines were created, including 3 negative controls for endogenous recombination (i.e., mock/empty vector, FNT, and Rag2 C terminus [R2CT]) and 2 positive controls (i.e., Rag2 core [R2CR] and wild-type Rag2 full length [R2FL]), as well as the 6 R2FL cell lines carrying the indicated PHD mutations. The cell lines were selected and harvested approximately 8–12 days after transduction, at which time genomic DNA was extracted, endogenous Ig rearrangement sequences were amplified by PCR, and then PCR products were analyzed by Southern blot as described (24, 34). With this approach, we examined IgH D-to-J and V-to-DJ rearrangements of VH families Q52 and 7183, as well as IgL Vκ-to-Jκ rearrangements (Figure 1B). We observed 3 distinct and reproducible trends among the mutants. The R2FL-W416L, -C446W, -W453R, and -C478Y mutations caused a marked defect in D-to-J rearrangements at the IgH locus and pronounced decreases in IgH V-to-DJ and IgL Vκ-to-Jκ rearrangements, whereas the R2FL-H481P mutation caused a milder defect in both IgH D-to-J and IgL Vκ-to-Jκ rearrangements and the R2FL-N474S mutant showed no obvious impairment in any rearrangement process when compared with wild-type R2FL. Of note, the R2FL-H481P mutant exhibited recombination activity similar to that of R2CR: near wild-type levels of IgH D-to-J rearrangements, a pronounced defect in completing the IgH V-to-DJ rearrangements, and a modest impairment in IgL Vκ-to-Jκ rearrangements, as previously described (35). Importantly, for all mutants that are defective in D-to-J rearrangement, the subsequent V-to-DJ defect could in part be explained by decreased substrate availability.

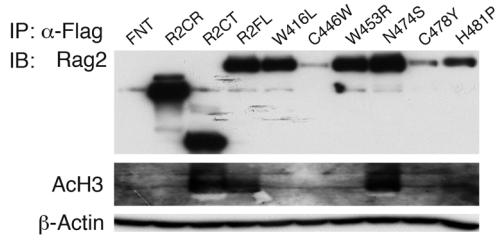

Figure 3
T-B-SCID/OS Rag2$_{PHD}$ mutations disrupt Rag2-histone interaction in pro-B cells. Anti-Flag IPs were performed on whole cell extracts from retrovirally transduced pro-B cells expressing constructs of interest: FNT tag, FNT-tagged core Rag2, C terminus of Rag2, R2FL, or full-length T-B-SCID/OS Rag2 mutants. Western immunoblotting analysis is shown for Rag2 and acetylated Histone H3 (AcH3). Flag IP loading was analyzed by Western blotting for β-actin on 1:1,000 input volume.

SCID/OS Rag2$_{PHD}$ mutations accelerate Rag2 degradation. Although the Rag2$_{PHD}$ has not been directly implicated in the posttranslational regulation of Rag2 expression, we wanted to exclude the possibility that the defects in endogenous recombination that we observed with several mutants could be simply due to abnormally low expression. Therefore, we investigated the relative abundance of all the mutants in the transduced pro-B cells, using Western blot of whole cell extracts (Figure 2A). Indeed, we observed that the relative amount of the R2FL-C446W mutant and -C478Y mutant proteins was greatly reduced compared to wild-type R2FL. The R2FL-W416L and -H481P mutants seemed to be present at somewhat lower amounts than wild-type R2FL, while the R2FL-W453R and -N474S mutants were comparable to wild type. Quantitative real-time PCR (Q-PCR) analyses of the corresponding mRNAs showed that the observed variations in steady-state protein abundance could not be accounted for by proportional changes in mRNA levels (Figure 2B). However, when the relative protein degradation rate was measured through a pulse-chase experiment, we observed a pronounced increase in the degradation rate of the R2FL-C446W and -C478Y mutants compared with wild-type R2FL, while the W453R and N474S mutations had little or no effect and the R2FL-W416L and -H481P mutants displayed an intermediate degradation rate (Figure 2C). Thus, the steady-state expression patterns of the mutants correlates with their degradation curves, and the expression defects that we observed seem to be due, at least in part, to increased protein degradation.

SCID/OS Rag2$_{PHD}$ mutations disturb Rag2 cellular localization. A previous study has identified a nonconsensus NLS sequence at the C-terminal end of Rag2 and showed that the PHD domain was not directly involved in the nuclear localization of Rag2 (19). Nevertheless, our constructs included a SV40 NLS sequence at the N terminus of Rag2, as a precaution to override any possible deleterious effects on nuclear transport due to mutations within the C-terminal region of the protein. To confirm whether this was the case, we analyzed Rag2 expression in the nuclear and cytoplasmic extracts from the retrovirally transduced pro-B cells. Like wild-type Rag2, R2FL-N474S and -H481P mutants were mainly expressed in the nucleus (Figure 2D). Unexpectedly, and despite the presence of the additional NLS, we found that 3 of the other mutants, R2FL-W416L, -C446W, and -W453R, were partly retained in the cytoplasm (Figure 2D). Most strikingly, the R2FL-W453R mutant, which was expressed at a high steady-state total abundance that was similar to wild-type Rag2, appeared to be mostly localized in the cytoplasm. These results clearly implicate the PHD domain in influencing the subcellular localization of Rag2.

SCID/OS Rag2$_{PHD}$ mutations disrupt interaction between Rag2 and histones. To characterize further the defects caused by the mutations within Rag2$_{PHD}$, we used a coimmunoprecipitation assay to investigate the histone binding properties of the mutants compared with wild-type Rag2, since the C terminus of Rag2, and specifically the PHD domain, has been shown to be required for histone interac-

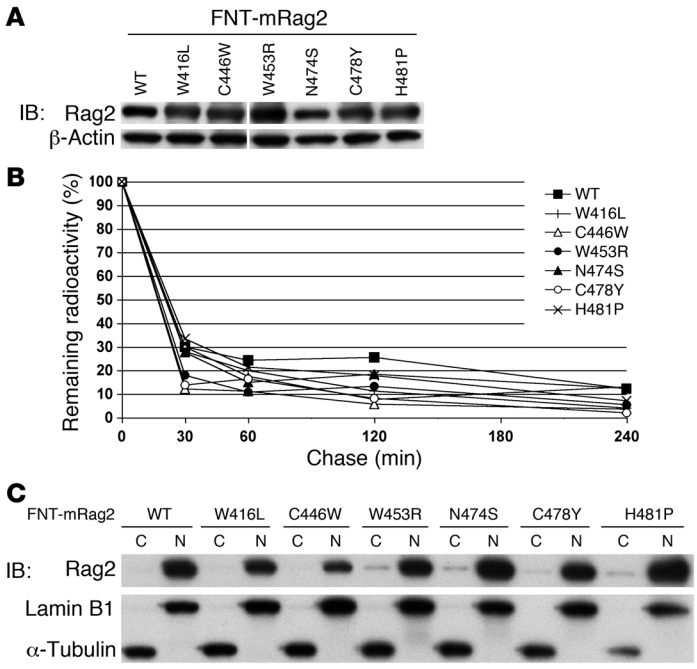

Figure 4
T-B-SCID/OS Rag2$_{PHD}$ mutants showed wild-type stability and cellular localization in 293T cells. (**A**) Whole cell extracts from 24-hour posttransfection 293T cells, coexpressing full-length mouse Rag1 and FNT-tagged full-length wild-type mouse Rag2 or full-length T-B-SCID/OS Rag2 mutants were analyzed by Western blotting for Rag2 and β-actin. The vertical line between FNT–mouse Rag2–C446W and –W453R is as in Figure 2A. (**B**) Transfected 293T cells were pulsed labeled with [^{35}S] methionine/cysteine to determine degradation of wild-type Rag2 and T-B-SCID/OS mutants. Radiolabeled proteins were IP at various times after pulse with anti-Rag2 antibody, fractionated by SDS PAGE, and quantified on a PhosphorImager. Data are normalized to the radioactivity levels at the end of pulse. (**C**) Cellular localization of Rag2 and T-B-SCID/OS mutants in 293T cells was determined by Western blotting analysis of fractionated cytoplasm and nuclear extracts (top). Purity and loading of the fractions were controlled by Western blotting for Lamin B1 (middle) and α-tubulin (bottom).

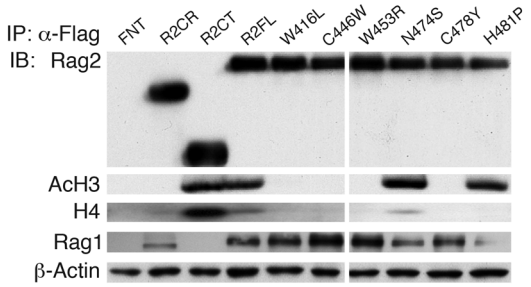

Figure 5
T-B-SCID/OS Rag2$_{PHD}$ mutations disrupt Rag2-histone interaction in 293T cells. Anti-Flag IPs were performed on whole cell extracts from 48-hour posttransfection cells coexpressing full-length Rag1 and constructs of interest: FNT tag, FNT-tagged core Rag2, C terminus of Rag2, R2FL, or full-length T-B-SCID/OS Rag2 mutants. Flag IPs were analyzed by Western immunoblotting for Rag2, acetylated Histone H3, Histone H4 (H4), or Rag1 and 1:1,000 input volume with anti–β-actin. Samples were loaded on the same gel, and the length of exposure was identical. The vertical line between mutants FNT–mouse Rag2–C446W and –aW453R is as in Figure 2A.

tion (24). Anti-Flag IPs of Rag2 proteins from retrovirally transduced pro-B cells confirmed the established interaction between the histones and the Rag2 C terminus, either alone or as part of full-length Rag2 (Figure 3). By comparison, the R2FL-N474S mutant interacted with the histones as well as wild-type Rag2, whereas the R2FL-H481P mutant interacted only weakly with the histones.

An obvious limitation of this approach was that for R2FL-W416L, -C446W, -W453R, and -C478Y mutants, analysis of histone interaction in B cells was complicated by inappropriate subcellular localization and/or decreased protein stability. For example, R2FL-W416L and -W453R mutants did not show any evidence of histone binding, but these proteins showed a low level of nuclear expression and would therefore not be expected to encounter histones as much as wild-type Rag2. Similarly, we could not conclude whether R2FL-C446W and -C478Y mutants had any histone binding capability, since they were expressed at very low levels and/or with inappropriate subcellular localization (Figure 2). For these reasons, we analyzed the histone binding properties of the panel of Rag2 proteins in 293T cells. In marked contrast to the pro-B cell line, we observed that Rag2 PHD mutants showed no difference in expression, degradation, or cellular localization, in comparison with wild-type Rag2, that could confound an interpretation (Figure 4). As in the previous figures, IPs were performed with anti-Flag antibodies on whole cell extracts from 293T cells cotransfected with full-length mouse Rag1 and the FNT-tagged Rag2 constructs, and samples were immunoblotted for Rag2, Rag1, and histones (Figure 5). Indeed, the 293T cell expression system confirmed the data from the B cell system, demonstrating the disruption of the interaction between Rag2 and the histones by the mutations involving the tryptophan and cysteine residues, i.e., W416L, C446W, W453R, and C478Y mutations. The R2FL-H481P mutant showed interaction with acetylated histone H3 (AcH3), while the R2FL-N474S mutant displayed a wild-type pattern of histone interactions with AcH3 and histone H4 (Figure 5).

Rag2-N474S mutant supports efficient V(D)J recombination. These analyses had not yet identified any particular defect associated with the N474S mutation. To determine whether there was any qualitative difference between the coding junctions induced by wild-type Rag2 and those induced by the R2FL-N474S mutant, we cloned and sequenced the PCR products obtained from endogenous heavy chain and light chain loci, rearranged in retrovirally transduced pro-B cells, as used previously for Southern blotting analysis in Figure 1B. We observed that the R2FL-N474S mutant induced endogenous IgH and Igκ rearrangements, presenting with features similar to those obtained with wild-type Rag2 (Supplemental Tables 1 and 2, respectively; supplemental material available online with this article; doi:10.1172/JCI41305DS1). Thus, the N474S mutation in the Rag2$_{PHD}$ does not affect the enzymatic steps subsequent to the initial DNA breaks generated by wild-type Rag1 and Rag2-N474S. Together with a previously published report (18), our data shows strong evidence that the N474S mutation may not be involved in the immunodeficiency developed by the patient.

Discussion

The C-terminal region of Rag2 contains a noncanonical PHD domain, whose integrity is critical to the physiological function of the Rag2 protein. Although dispensable for catalysis, it is known that this region interacts with histones (24) and, via the PHD domain, binds preferentially to H3K4me3 (25, 26). Based on the analysis of the W453R mutant, it was proposed that disruption of this contact severely disabled Rag2 and was alone responsible for the resulting profound immunodeficiency (25, 26). Our study confirms that histone contacts indeed depend upon this region and can be important for Rag2 function. However, we also show that the PHD domain has a more global effect on the structure of the entire Rag2 protein not previously revealed from other studies. Our findings now suggest that even though mutations in the PHD domain may indeed render the protein unable to stably interact with histones, the overriding functional defect in these mutants is their mislocalization and/or heightened destabilization and degradation (Supplemental Table 3). Our data point to multiple levels of the regulation of Rag2 protein metabolism, and results obtained from nonlymphoid cell systems must be interpreted conservatively and with caution.

As shown in Figure 1A, the PHD domain coordinates 2 zinc ions by residues C419, C423, C446, H452, H455, C458, C478, and H481 (17, 18, 25). Mutations in the zinc anchor residues, C446, C478, and H481 that are found in SCID/OS patients, are clearly deleterious and strongly suggest that zinc coordination is crucial for the function of Rag2. Our studies show that C446W and C478Y mutations most severely impair the stability of Rag2, as evidenced by rapid degradation of these proteins compared with wild type. We hypothesize that these mutations severely disrupt zinc binding and, subsequently, the folding of the PHD domain, which affects the overall structural integrity of Rag2. Thus, for patients carrying these mutations, the resultant Rag2 protein instability seems to be sufficient to explain the recombination defect. Following the same reasoning, the H481P mutation of another zinc anchor residue and the W416L mutation nearby the zinc anchor residue C419 would similarly also lead to misfolding of the PHD domain, resulting in the observed increased degradation rate, albeit lower than the previous. Interestingly, W416 (and nearby C419) and H481 are localized at the very N- and C-terminal ends of the PHD domain, respectively (18, 25), which may explain the less dramatic effect of these point mutations when compared with mutations of anchor residues deeper within the PHD finger. Alternatively, it is also possible that these mutations may disturb the stability of Rag2

indirectly, through an effect on the nearby phosphorylation site at T490 or on the cationic region spanning residues 499–508, which were both shown to govern Rag2 degradation (20–23).

In either case, the severely impaired behavior of these 2 mutants can also be explained, at least in part, by decreased protein stability. In contrast, the properties of the W453R mutant suggest that when the stability of Rag2 is not affected, mutation in the PHD domain may still affect other domains in the vicinity and alter their functions. Accordingly, we suggest that the W453R mutation might not disrupt the integrity of the PHD domain to such an extent as to trigger degradation of Rag2 but nevertheless affects the nearby NLS, leading to the retention of Rag2 into the cytoplasm. Structural evidence to support this model must await crystallographic data for the Rag2 full-length protein.

Interestingly, the effects of the SCID/OS mutations on stability and cellular compartmentalization of Rag2 appear to be cell-type specific, since differences in protein stability and subcellular localization observed in pro-B cells were not evident in 293T cells. Even when wild-type protein levels and proper nuclear localization of the Rag2 mutants was achieved by overexpression in 293T cells, most of them failed to bind with histones. While our study does not differentiate direct and indirect interactions between Rag2 and histones, it supports the hypothesis that Rag2 interaction with histones is a process associated with the structural properties of the PHD domain.

The observation that there were marked differences in Rag2 protein metabolism between pro-B cells and 293T cells is relevant in interpreting structure/function data and may be important in revealing how Rag protein activity and V(D)J recombination are regulated in lymphocytes. Nevertheless, the underlying mechanism is not known. There are several differences between the 2 systems that may be relevant. Differences may be a consequence of the overexpression achieved in 293T cells that overrides pathways that would otherwise target them for destruction. Another possibility is that the thioredoxin tag on the N terminus of Rag2 constructs may improve the stability of the proteins in human cells but not in mouse cells. Such species specificity may also be pertinent with respect to the ability of the SV40 NLS included in the N-terminal tag to drive expression of Rag2 and the SCID/OS mutants into the nucleus of the 293T cells, while it seems to do so inefficiently in mouse pro-B cells, in which nuclear localization may rely mostly on the intrinsic NLS in the C-terminal of Rag2. In this way, our comparative analysis highlights the differences of the cellular systems used to study the function of the factors involved in V(D)J recombination.

We expect the pro-B cell system to more closely match physiology of developing lymphocytes than the 293T cell system, as pro-B cells are predicted to contain regulatory activities specific to the immunological processes that would be lacking in 293T cells. However, the pro-B cell system still doesn't recapitulate the environmental influences that may lead to the development of OS from some hypomorphic mutations and T-B-SCID from others. With that in mind, it may be that the development of either OS or T-B-SCID is not solely associated with the level of recombination achieved by the Rag2 mutants in these model systems. Indeed, we showed that the Rag2-H481P mutant retains partial recombination activity, in correlation with phenotypical features of the patient that presents some Ig rearrangements in bone marrow cells while the patient was diagnosed with T-B-SCID (31). On the contrary, other mutations leading to severely impaired recombination on endogenous loci in our pro-B cell system were isolated from OS patients. A comparative in vivo study of knockin mouse models of representative mutations could help to determine the requirements for the development of OS versus T-B-SCID. Such studies may reveal the developmental or environmental pressures that would explain why the same mutation would lead to OS in one patient and to T-B-SCID in another, as it is the case for the W416L mutation (32).

We provide the first set of data to our knowledge that would explain, at least in part, why the immunodeficiency triggered by some $Rag2_{PHD}$ point mutants is stronger compared with the effects of the deletion of the whole C-terminal domain of Rag2, highlighted by the studies of the core Rag2 knockin mouse (35, 36). Rag2 core is likely to be mainly expressed into the nucleus, in which it allows initiation of V(D)J recombination. In contrast, point mutations in the PHD domain can affect the subcellular localization and stability of Rag2, rendering them unable to reach their DNA target and participate in V(D)J recombination. W416L and H481P mutations illustrate how we imagine the different effects of the mutations on Rag2 metabolism are brought to bear on the mutants' defective behavior. The Rag2-W416L mutant is not as stable as wild-type Rag2 and is partly retained in the cytoplasm, which is evident in the decrease in D-to-J rearrangements. The Rag2-H481P mutant shows a similarly reduced stability but a higher level of D-to-J recombination that may be explained by its full expression into the nucleus. It is important to note that, despite that capability, it is unable to assist the completion of the IgH rearrangements, like core Rag2. Interestingly, H481P did not show a complete loss of interaction with histones. This observation supports the notion that specific histone contacts, such as with H3K4me3, may be important or that other non-histone–related interactions are relevant and affected by the mutations that have yet to be identified.

Finally, our present study confirms that the N474S mutation may have no deleterious effect on Rag2 function, in accordance with a previous report (18). Therefore, that particular mutation may not be implicated in the immunodeficiency developed by the patient. It is important to note that this mutation was described before the discovery of NHEJ factors such as Cernunnos-XLF or Artemis, defects which have been demonstrated in human immunodeficiencies such as SCID or OS (7, 37–39). Thus, one model to explain the immunodeficiency developed by the patient is that this individual had mutations in these or another gene encoding a protein that has yet to be identified as a factor involved in lymphogenesis. Another exciting possibility is that the effect of the N474S mutation is affecting yet another regulatory function that remains to be defined and that may not be detected in our cellular system.

In summary, our work reveals that point mutations in the $Rag2_{PHD}$ can reduce protein stability and lead to altered subcellular localization. We have also expanded the number of Rag2 PHD mutants that have been shown to affect histone interaction. These results have important implications for studying posttranslational regulatory mechanisms that govern antigen receptor gene assembly.

Methods

Reagents. The following primary antibodies were used: anti-Flag (catalog F-3165; Sigma-Aldrich), anti-Rag1 (catalog 5599; Santa Cruz Biotechnology Inc.), anti–β-Actin (catalog AC74; Sigma-Aldrich), anti–α-Tubulin (B512; Sigma-Aldrich), anti-Lamin B1 (6216; Santa Cruz Biotechnology Inc.), anti–acetyl-Histone H3 (06-599; Upstate Biotechnology), and Histone H4 (07-108; Upstate Biotechnology). Polyclonal anti-Rag2 was generated as

described previously (40). Secondary HRP-conjugated anti-mouse and anti-rabbit IgG were from Pierce, and anti-Goat was from Santa Cruz Biotechnology Inc. Flag peptide and anti-Flag beads were from Sigma-Aldrich.

Expression vectors and mutagenesis. Retroviral vectors were as described previously (24). Mutagenesis was done with QuikChange II XL Site-Directed Mutagenesis Kit (Stratagene). For 293T cell expression, BamHI-NotI fragments from the retroviral vectors containing mouse Rag2 sequences were cloned into pEF plasmid.

Cell culture. Cells were maintained at 37°C and 5% CO_2. *Rag2*$^{-/-}$ murine pro-B cells were cultured in RPMI 1640 (Gibco) with 10% fetal bovine serum (Sigma-Aldrich), 2 mM L-glutamine, 1 mM Na-pyruvate, 1% antibiotic-antimycotic (Invitrogen), and 50 μM β-Mercaptoethanol (Sigma-Aldrich). 293T cells were grown in Dulbecco's modified Eagle's medium (Cellgro) with 10% bovine calf serum (Hyclone), 2 mM L-glutamine, 1 mM Na-pyruvate, and 1% antibiotic-antimycotic (Invitrogen).

Retroviral transduction. The Abelson-transformed *Rag2*$^{-/-}$ murine pro-B cell line was created by infection of bone marrow cells from adult *Rag2*$^{-/-}$ mice (41) with v-abl virus as previously described (42). Animal care and use for this experiment was approved by the Institutional Animal Care and Use Committee of the Rockefeller University. The *Rag2*$^{-/-}$ mice were a gift from the laboratory of Fred Alt, Harvard Medical School, Boston, Massachusetts. The pro-B cells were retrovirally transduced, also as previously described (24). In brief, 293T cells were cotransfected by the calcium phosphate method with 10 μg retroviral vector carrying the gene of interest, 5 μg pMD.G vector, which encodes vesicular stomatitis G protein, and 7.5 μg pMD.OGP vector, which encodes MoMLV gag-pol (43). Media was changed 24 hours after transfection for 293T cell growth medium supplemented with 50 μM β-Mercaptoethanol (Sigma-Aldrich). Supernatant was collected 48 hours after transfection, filtered, supplemented with polybrene at 5 μg/ml, and used to resuspend *Rag2*$^{-/-}$ murine pro-B cells at 0.6 millions/ml. After 24 hours transduction, media was changed and cells were selected with 1.5 μg/ml puromycin.

Expression into 293T cells. 293T cells were cotransfected by the calcium phosphate method, with 5 μg pEF vector carrying *Rag2* gene of interest and 7 μg pEBB-Rag1 vector.

Southern blotting and sequence analyses. Isolation of genomic DNA, PCRs, and Southern blotting analyses were performed as described previously (24). PCR products were cloned into pGEM-T Easy vector (Promega) and sequencing was performed by Mount Sinai School of Medicine DNAcore facility.

IP. Whole cell extract was prepared in lysis Buffer A-500 (25 mM Tris-HCl [pH 8.0], 500 mM KCl, 0.5 mM EDTA, 10% glycerol, 1 mM DTT, 0.05% Triton X-100) and sonicated. For IP, whole cell extract was treated with DNAseI at 80 μg/ml for 30 minutes, followed by 30 minutes with ethidium bromide at 200 μg/ml. After centrifugation, the supernatant was incubated with anti-Flag beads overnight, followed by washings with Buffer A-500 and elution in the following elution buffer: 20 mM Tris-HCl (pH 7.5), 300 mM NaCl, 0.2 mM EDTA, 0.1% NP-40, 15% glycerol, 0.2 mg/ml Flag peptide. For Rag2 IP, the supernatant was precleared with 1.5 μg/ml rabbit IgG (Pierce) for 1 hour and incubated with protein G sepharose 4 Fast Flow beads (Amersham) for 1 hour. After centrifugation, the supernatant was incubated with anti-Rag2 antibody overnight, then with protein G sepharose 4 Fast Flow beads (Amersham) for 1 hour, followed by washings with Buffer A-500 and elution in buffer A-0 (25 mM Tris-HCl [pH 8.0], 0.5 mM EDTA, 10% glycerol, 1 mM DTT, 0.05% Triton X-100). Samples were complemented with loading dye buffer (100 mM Tris-HCl [pH 6.8], 10% glycerol, 100 mM DTT, 2% SDS, 0.1 mM Bromophenol Blue).

Fractionation. Cells were resuspended in RSB Buffer (20 mM Tris-HCl [pH 7.5], 10 mM NaCl, 5 mM $MgCl_2$, 1 mM PMSF), complemented with 0.5% NP-40, and incubated on ice for 2 minutes. After centrifugation, supernatant containing cytoplasmic fraction was harvested, and the nuclei pellet was washed twice with RSB Buffer, before lysis in Buffer A-500 and sonication.

Western blotting analysis. Whole cell extracts, nuclear/cytoplasmic fractions, and IPs were separated on 4%–20% or 8%–16% SDS-PAGE gradient gels (Bio-Rad). Proteins were transferred to PVDF membrane (Bio-Rad) and detected following standard protocol.

Q-PCR. Total RNA was extracted from retrotransduced pro-B cells using the RNeasy Mini Kit (Qiagen), according to the manufacturer's instructions. Q-PCR was performed as described previously (44). The primers used to amplify FNT-tagged *Rag2* mRNA were across the FNT tag region: FNT-F (5′-CGTTGCAAAACTGAACATCGA-3′) and FNT-R (5′-GGATACCACG-GATGCCATATTT-3′). The fold enrichment of each amplified fragment was determined relative to ubiquitin (*Ubr1*) mRNA amplification and then normalized to that of FNT-tagged full-length wild-type mouse Rag2.

Pulse-chase assay. Cells were starved for 30 minutes in methionine/cysteine-free Dulbecco's modified Eagle's medium (Gibco) supplemented with 10% Dialysed Fetal Bovine Serum (Gibco), 2 mM L-glutamine, and 1 mM Na-pyruvate (Invitrogen), then labeled with 20 μCi/ml [^{35}S]Methionine/[^{35}S]Cysteine Labeling Mix (Perkin Elmer) for 30 minutes. Radioactivity was chased in starvation media supplemented with 2 mM L-Methionine (Sigma-Aldrich), 2 mM L-Cysteine (Fluka), and 10 μg/ml Cyclohexamide (Sigma-Aldrich) for 30 minutes, 1 hour, 2 hours, 4 hours, or 8 hours. Anti-Rag2 IPs were prepared as described above and separated on 10% SDS-PAGE gels. [^{35}S]Rag2 was quantified with a PhosphorImager (Molecular Dynamics).

For the new mutation described in this study (C446W), the patient sample used to evaluate the Rag2 mutation was obtained after the parents provided informed consent, and the study was approved by the Great Ormond Street Hospital Research Ethics Committee.

Acknowledgments

We thank Alexandre Garin and Sergio Lira for advice on Q-PCR and Juan Carcamo and members of the Cortes laboratory for suggestions and critical reading of the manuscript. Work in the P. Cortes laboratory is in part supported by NIH Program Project grant P01 AI61093, the Irma T. Hirsch/Monique Weill-Caullier Research Award, and past support from the NIH (R56AI070532-01A1), as well as the American Cancer Society (RSG-04-191-01 LIB), and a Leukemia and Lymphoma Society Scholar Award. We also acknowledge the support of Fondazione Cariplo N.O.B.E.L. grant (to P. Vezzoni and A. Villa) and Italian Telethon Foundation (to A. Villa) and FIRB/MIUR (RBINO4CHXT to P. Vezzoni).

Received for publication September 30, 2009, and accepted in revised form January 20, 2010.

Address correspondence to: Patricia Cortes, Department of Medicine, Mount Sinai School of Medicine, 1425 Madison Avenue, Room 12-23B, New York, NY 10029. Phone: 212.659.9443; Fax: 212.849.2525; E-mail: Patricia.Cortes@mssm.edu.

Chrystelle Couëdel's present address is: Department of Immunology and Molecular Pathology, Division of Infection and Immunity, University College London, United Kingdom.

1. Schatz DG, Oettinger MA, Baltimore D. The V(D)J recombination activating gene, RAG-1. *Cell*. 1989; 59(6):1035–1048.
2. Oettinger MA, Schatz DG, Gorka C, Baltimore D. RAG-1 and RAG-2, adjacent genes that synergistically activate V(D)J recombination. *Science*. 1990; 248(4962):1517–1523.
3. Soulas-Sprauel P, et al. V(D)J and immunoglobulin class switch recombinations: a paradigm to study the regulation of DNA end-joining. *Oncogene*. 2007; 26(56):7780–7791.
4. Puebla-Osorio N, Zhu C. DNA damage and repair

during lymphoid development: antigen receptor diversity, genomic integrity and lymphomagenesis. *Immunol Res*. 2008;41(2):103–122.
5. Alt FW, et al. Ordered rearrangement of immunoglobulin heavy chain variable region segments. *EMBO J*. 1984;3(6):1209–1219.
6. Villa A, Santagata S, Bozzi F, Imberti L, Notarangelo LD. Omenn syndrome: a disorder of Rag1 and Rag2 genes. *J Clin Immunol*. 1999;19(2):87–97.
7. Ege M, et al. Omenn syndrome due to ARTEMIS mutations. *Blood*. 2005;105(11):4179–4186.
8. Grunebaum E, Bates A, Roifman CM. Omenn syndrome is associated with mutations in DNA ligase IV. *J Allergy Clin Immunol*. 2008;122(6):1219–1220.
9. Sobacchi C, Marrella V, Rucci F, Vezzoni P, Villa A. RAG-dependent primary immunodeficiencies. *Hum Mutat*. 2006;27(12):1174–1184.
10. Silver DP, Spanopoulou E, Mulligan RC, Baltimore D. Dispensable sequence motifs in the RAG-1 and RAG-2 genes for plasmid V(D)J recombination. *Proc Natl Acad Sci U S A*. 1993;90(13):6100–6104.
11. Cuomo CA, Oettinger MA. Analysis of regions of RAG-2 important for V(D)J recombination. *Nucleic Acids Res*. 1994;22(10):1810–1814.
12. Sadofsky MJ, Hesse JE, Gellert M. Definition of a core region of RAG-2 that is functional in V(D)J recombination. *Nucleic Acids Res*. 1994;22(10):1805–1809.
13. Kim DR, Dai Y, Mundy CL, Yang W, Oettinger MA. Mutations of acidic residues in RAG1 define the active site of the V(D)J recombinase. *Genes Dev*. 1999; 13(23):3070–3080.
14. Swanson PC, Desiderio S. V(D)J recombination signal recognition: distinct, overlapping DNA-protein contacts in complexes containing RAG1 with and without RAG2. *Immunity*. 1998;9(1):115–125.
15. Jones JM, Simkus C. The roles of the RAG1 and RAG2 "non-core" regions in V(D)J recombination and lymphocyte development. *Arch Immunol Ther Exp (Warsz)*. 2009;57(2):105–116.
16. Kirch SA, Rathbun GA, Oettinger MA. Dual role of RAG2 in V(D)J recombination: catalysis and regulation of ordered Ig gene assembly. *EMBO J*. 1998; 17(16):4881–4886.
17. Callebaut I, Mornon JP. The V(D)J recombination activating protein RAG2 consists of a six-bladed propeller and a PHD fingerlike domain, as revealed by sequence analysis. *Cell Mol Life Sci*. 1998;54(8):880–891.
18. Elkin SK, et al. A PHD finger motif in the C terminus of RAG2 modulates recombination activity. *J Biol Chem*. 2005;280(31):28701–28710.
19. Corneo B, Benmerah A, Villartay JP. A short peptide at the C terminus is responsible for the nuclear localization of RAG2. *Eur J Immunol*. 2002;32(7):2068–2073.
20. Lin WC, Desiderio S. Regulation of V(D)J recombination activator protein RAG-2 by phosphorylation. *Science*. 1993;260(5110):953–959.
21. Li Z, Dordai DI, Lee J, Desiderio S. A conserved degradation signal regulates RAG-2 accumulation during cell division and links V(D)J recombination to the cell cycle. *Immunity*. 1996;5(6):575–589.
22. Lee J, Desiderio S. Cyclin A/CDK2 regulates V(D)J recombination by coordinating RAG-2 accumulation and DNA repair. *Immunity*. 1999;11(6):771–781.
23. Ross AE, Vuica M, Desiderio S. Overlapping signals for protein degradation and nuclear localization define a role for intrinsic RAG-2 nuclear uptake in dividing cells. *Mol Cell Biol*. 2003;23(15):5308–5319.
24. West KL, et al. A direct interaction between the RAG2 C terminus and the core histones is required for efficient V(D)J recombination. *Immunity*. 2005;23(2):203–212.
25. Ramon-Maiques S, et al. The plant homeodomain finger of RAG2 recognizes histone H3 methylated at both lysine-4 and arginine-2. *Proc Natl Acad Sci U S A*. 2007;104(48):18993–18998.
26. Matthews AG, et al. RAG2 PHD finger couples histone H3 lysine 4 trimethylation with V(D)J recombination. *Nature*. 2007;450(7172):1106–1110.
27. Liu Y, et al. A plant homeodomain in RAG-2 that binds Hypermethylated lysine 4 of histone H3 is necessary for efficient antigen-receptor-gene rearrangement. *Immunity*. 2007;27(4):561–571.
28. Shimazaki N, Tsai AG, Lieber MR. H3K4me3 stimulates the V(D)J RAG complex for both nicking and hairpinning in trans in addition to tethering in cis: implications for translocations. *Mol Cell*. 2009; 34(5):535–544.
29. Gomez CA, et al. Mutations in conserved regions of the predicted RAG2 kelch repeats block initiation of V(D)J recombination and result in primary immunodeficiencies. *Mol Cell Biol*. 2000;20(15):5653–5664.
30. Villa A, et al. V(D)J recombination defects in lymphocytes due to RAG mutations: severe immunodeficiency with a spectrum of clinical presentations. *Blood*. 2001;97(1):81–88.
31. Noordzij JG, et al. The immunophenotypic and immunogenotypic B-cell differentiation arrest in bone marrow of RAG-deficient SCID patients corresponds to residual recombination activities of mutated RAG proteins. *Blood*. 2002;100(6):2145–2152.
32. Haq IJ, et al. GvHD-associated cytokine polymorphisms do not associate with Omenn syndrome rather than T-B- SCID in patients with defects in RAG genes. *Clin Immunol*. 2007;124(2):165–169.
33. Ktiouet S, et al. Omenn syndrome due to mutation of the RAG2 gene [Published online ahead of print March 11, 2009]. *J Eur Acad Dermatol Venereol*. doi:10.1111/j.1468-3083.2009.03232.x.
34. Schlissel MS, Corcoran LM, Baltimore D. Virus-transformed pre-B cells show ordered activation but not inactivation of immunoglobulin gene rearrangement and transcription. *J Exp Med*. 1991;173(3):711–720.
35. Akamatsu Y, et al. Deletion of the RAG2 C terminus leads to impaired lymphoid development in mice. *Proc Natl Acad Sci U S A*. 2003;100(3):1209–1214.
36. Curry JD, Schlissel MS. RAG2's non-core domain contributes to the ordered regulation of V(D)J recombination. *Nucleic Acids Res*. 2008;36(18):5750–5762.
37. Moshous D, et al. Artemis, a novel DNA double-strand break repair/V(D)J recombination protein, is mutated in human severe combined immune deficiency. *Cell*. 2001;105(2):177–186.
38. Buck D, et al. Cernunnos, a novel nonhomologous end-joining factor, is mutated in human immunodeficiency with microcephaly. *Cell*. 2006;124(2):287–299.
39. Ahnesorg P, Smith P, Jackson SP. XLF interacts with the XRCC4-DNA ligase IV complex to promote DNA nonhomologous end-joining. *Cell*. 2006; 124(2):301–313.
40. Spanopoulou E, et al. Localization, interaction, and RNA binding properties of the V(D)J recombination-activating proteins RAG1 and RAG2. *Immunity*. 1995;3(6):715–726.
41. Shinkai Y, et al. RAG-2-deficient mice lack mature lymphocytes owing to inability to initiate V(D)J rearrangement. *Cell*. 1992;68(5):855–867.
42. Roman CA, Cherry SR, Baltimore D. Complementation of V(D)J recombination deficiency in RAG-1($^{-/-}$) B cells reveals a requirement for novel elements in the N-terminus of RAG-1. *Immunity*. 1997;7(1):13–24.
43. He KL, Ting AT. A20 inhibits tumor necrosis factor (TNF) alpha-induced apoptosis by disrupting recruitment of TRADD and RIP to the TNF receptor 1 complex in Jurkat T cells. *Mol Cell Biol*. 2002; 22(17):6034–6045.
44. Martin AP, et al. The chemokine binding protein M3 prevents diabetes induced by multiple low doses of streptozotocin. *J Immunol*. 2007;178(7):4623–4631.